

Tipping points for seawater intrusion in coastal aquifers under rising sea level

This article has been downloaded from IOPscience. Please scroll down to see the full text article.

2013 Environ. Res. Lett. 8 014001

(<http://iopscience.iop.org/1748-9326/8/1/014001>)

View [the table of contents for this issue](#), or go to the [journal homepage](#) for more

Download details:

IP Address: 131.94.16.64

The article was downloaded on 11/01/2013 at 17:11

Please note that [terms and conditions apply](#).

Tipping points for seawater intrusion in coastal aquifers under rising sea level

Katerina Mazi^{1,2,3}, Antonis D Koussis^{2,3} and Georgia Destouni^{1,3}

¹ Department of Physical Geography and Quaternary Geology, Bert Bolin Centre for Climate Research, Stockholm University, Sweden

² Institute for Environmental Research and Sustainable Development, National Observatory of Athens, Greece

³ Navarino Environmental Observatory, Messinia, Greece

E-mail: kmazi@noa.gr

Received 16 July 2012

Accepted for publication 10 December 2012

Published 9 January 2013

Online at stacks.iop.org/ERL/8/014001

Abstract

This study considers different projections of climate-driven sea-level rise and uses a recently developed, generalized analytical model to investigate the responses of sea intrusion in unconfined sloping coastal aquifers to climate-driven sea-level rise. The results show high nonlinearity in these responses, implying important thresholds, or tipping points, beyond which the responses of seawater intrusion to sea-level rise shift abruptly from a stable state of mild change responses to a new stable state of large responses to small changes that can rapidly lead to full seawater intrusion into a coastal aquifer. The identified tipping points are of three types: (a) spatial, for the particular aquifers (sections) along a coastline with depths that imply critical risk of full sea intrusion in response to even small sea-level rise; (b) temporal, for the critical sea-level rise and its timing, beyond which the change responses and the risk of complete sea intrusion in an aquifer shift abruptly from low to very high; and (c) managerial, for the critical minimum values of groundwater discharge and hydraulic head that inland water management must maintain in an aquifer in order to avoid rapid loss of control and complete sea intrusion in response to even small sea-level rise. The existence of a tipping point depends on highly variable aquifer properties and groundwater conditions, in combination with more homogeneous sea conditions. The generalized analytical model used in this study facilitates parsimonious quantification and screening of sea-intrusion risks and tipping points under such spatio-temporally different condition combinations along extended coastlines.

Keywords: sloping coastal aquifer, seawater intrusion, sea-level rise, sharp interface, tipping points

 Online supplementary data available from stacks.iop.org/ERL/8/014001/mmedia

1. Introduction

About 70% of the world population lives within a day's walk from the coast (Brown *et al* 2002). Many of these often densely populated coastal zones rely on groundwater for

drinking and for their economies. Especially in semiarid/arid regions, aquifers are essential water sources, vulnerable to climate change. Therefore the management of coastal water resources should consider climate-change impacts; indeed, related hydrologic studies have gained importance after IPCC's Fourth Assessment Report (Bates *et al* 2008).

Projected climatic changes influence the seaside and/or inland boundary conditions of coastal aquifers, as well as the salinity of lakes and enclosed seas to which aquifers



Content from this work may be used under the terms of the [Creative Commons Attribution-NonCommercial-ShareAlike 3.0 licence](http://creativecommons.org/licenses/by-nc-sa/3.0/). Any further distribution of this work must maintain attribution to the author(s) and the title of the work, journal citation and DOI.

discharge. Large-scale changes in these boundary conditions further influence flow and pressure distributions in multiple regional aquifers, leading to large-scale, even though spatially variable changes in sea intrusion over long coastlines (Jarsjö and Destouni 2004, Shibuo *et al* 2006). Sea intrusion, exacerbated by intensive exploitation, threatens coastal aquifers with large-scale and slow-to-reverse contamination: mixing 2% seawater (salinity 35000 ppm TDS) with freshwater makes the mixture non-potable (standard 500 ppm TDS) and 5%-mixing makes it unfit for irrigation (Custodio and Bruggeman 1987). While large-scale changes in these mixing conditions threaten main freshwater sources for many people in densely populated coastal regions, the coastal groundwater flows that determine the mixing conditions are among the least well monitored and most uncertain environmental flows (Destouni *et al* 2008, Prieto and Destouni 2011).

This study considers the sea-level rise projections of IPCC (Bates *et al* 2008) and AMAP (2011) and uses the generalized analytical solution of Koussis *et al* (2012) to investigate the sea-intrusion responses in unconfined coastal aquifers to climate-driven scenarios of sea-level rise. The generalization achieved by Koussis *et al* (2012) is to account for the generally present (e.g., for the Mediterranean aquifers of: Nile Delta 0.3%, Israeli Coastal 1%, Akrotiri, Cyprus 1.7%) and usually hydraulically significant aquifer slope (Carrera *et al* 2010) that has previously been ignored in analytical sharp-interface solutions of seawater intrusion (e.g., Custodio 1987a, 1987b, Strack 1976) and in their applications (e.g., Werner and Simmons 2009, Ferguson and Gleeson 2012). Koussis *et al* (2012) extended the Strack (1976)–Girinskii (1947) discharge potential approach to steady interface flow in *sloping* phreatic aquifers by approximating the gravity-driven flow component. In that formulation, the aquifer geometry is represented in a schematized yet realistic manner, whereas modelling an inclined aquifer as horizontal requires subjective positioning of a fictitious horizontal base (see further discussion in supplemental material (SM) 1 available at stacks.iop.org/ERL/8/014001/mmedia).

This conceptualization allows for an elegant, generalized aquifer representation and credible flow behaviour, suitable for regional-scale management studies of coastal groundwater resources (e.g., like those in Koussis *et al* 2010a, 2010b). The objective of the present study is to analyse systematically, with this new model, how interface flow and sea intrusion in unconfined coastal aquifers respond to different scenarios of sea-level rise, subject to different inland boundary conditions and aquifer coastline depths, for multiple slope and hydraulic conductivity realizations relevant for various regional conditions and coastal aquifers. We focus on high response nonlinearity, implying important thresholds, or *tipping points*, at which seawater intrusion responses to sea-level rise shift abruptly from a stable state of mild change responses, to a new stable state of large responses to small changes, leading to rapid seawater intrusion up to complete aquifer invasion. Coastal aquifers should be managed so that flow conditions do not approach these thresholds.

2. Methodology and theory

We consider here both *flux-* and *head-control* conditions for the coastal aquifer (Werner and Simmons 2009). Flux control implies that the submarine outflow of fresh groundwater remains constant; in practice, this can be achieved by adjusting the upstream groundwater management. Head control implies instead that the groundwater hydraulic head remains constant at the inland boundary; in practice, this can be achieved through connection to a regulated surface water body, ensuring a certain stage at that boundary. How relevant and realistic these concepts are must be assessed in each field case. For both control cases holds that the head profile has a maximum (groundwater divide) located no farther from the coastline than the control section; the freshwater flow reaching the coast, $|q_0|$, is thus the product of recharge rate, r , and the distance of the groundwater divide from the coastline, ℓ_{div} ($|q_0| = r \times \ell_{\text{div}}$). In the flux-control case (fixed q_0), this implies that, when the sea-level changes, the maximum head changes also, but the groundwater divide remains fixed (fixed length of recharge). Conversely, in the head-control case, the position of the groundwater divide shifts seawards in response to a rising sea level, to maintain the given inland boundary head; consequently the fresh-water outflow to the sea diminishes.

Consider, then, steady flow, with a fresh-sea water interface, in an unconfined *shallow* aquifer (Dupuit–Forchheimer approximation: static pressure, hence uniform potential and specific discharge over aquifer depth) with hydraulic conductivity (K), resting on an inclined (angle φ against the horizontal) impervious base, and being recharged uniformly at the rate r (see schematic figure A1 in SM 1 available at stacks.iop.org/ERL/8/014001/mmedia). The position (ℓ) axis follows the aquifer base, from the vertical projection of the intersection of the sea level and the coast, at the depth H_{sea} from the sea surface to the aquifer base, where the datum is placed. The depth normal to the aquifer base is h , the z -axis is vertical, and the hydraulic head is $\phi = h \cos \varphi + z_b$, with z_b being the bed elevation; $dz_b/d\ell = \sin \varphi$. The sea constitutes a constant-head boundary of the aquifer, with hydraulic head $\phi(\ell = 0) = H_{\text{sea}}$. Koussis *et al* (2012) use a discharge potential for the gravity-driven flow in which the depth is approximated as a constant h_0 (i.e., the gravity-driven flow— $Kh \sin \varphi \approx -Kh_0 \sin \varphi$), and assume that the freshwater flows over a stagnant seawater wedge. We refer to that paper for the theory leading to the equations used here. SM 1 (available at stacks.iop.org/ERL/8/014001/mmedia) presents a reprise of that theory, with extensions; the main resulting equations used in the present study are summarized below.

The equation governing the flow in the entire aquifer is $d^2\Phi/d\ell^2 = -r \cos \varphi \approx -r$, with the discharge potential Φ defined differently in the freshwater zone 1 and in the interface zone 2 (see SM1, figure A1 and equations S4, S6 available at stacks.iop.org/ERL/8/014001/mmedia). Integrating and implementing the boundary conditions for flux control and for head control yield the discharge potential at the sea-intrusion toe, lead in the flux-control case to the quadratic equation (1) and in the head-control case to

the cubic equation (2) for the location of the sea intrusion toe ℓ_T :

$$\begin{aligned}
 & [r + K\delta(1 + \delta)\sin^2\varphi]\ell_T^2 + 2[q_0 - K\delta(1 + \delta)\sin\varphi H_{\text{sea}}]\ell_T \\
 & + K\delta(1 + \delta)H_{\text{sea}}^2 = 0 \tag{1} \\
 & (1 + \delta)\sin^2\varphi\ell_T^3 + \left\{ \frac{r\ell_{\text{control}}}{K} \right. \\
 & + \sin\varphi [2h_0 - (1 + \delta)(2H_{\text{sea}} - \delta\ell_{\text{control}}\sin\varphi)] \left. \right\} \ell_T^2 \\
 & - \left[\frac{r\ell_{\text{control}}^2}{K} + h_{\text{control}}^2 - (1 + \delta)H_{\text{sea}}^2 \right. \\
 & + 2\sin\varphi\ell_{\text{control}}[h_0 + H_{\text{sea}}\delta(1 + \delta)] \left. \right] \ell_T \\
 & + \ell_{\text{control}}\delta(1 + \delta)H_{\text{sea}}^2 = 0 \tag{2}
 \end{aligned}$$

where $\delta = (\rho_s - \rho_f)/\rho_f$, with ρ_s and ρ_f the respective salt- and fresh-water densities, and $\phi(\ell_{\text{control}}) = h(\ell_{\text{control}}) + \sin\varphi\ell_{\text{control}}$ the hydraulic head at the inland boundary. Only the root with the negative square root has physical meaning for equation (1). The single meaningful root of equation (2) lies on the branch of the function $\ell_T(H_{\text{sea}})$ on which ℓ_T increases as H_{sea} increases and is the smaller of the two positive roots (a negative root is rejected).

The critical condition at which the seawater is on the verge of invading the entire aquifer occurs when the interface toe reaches the groundwater divide, where the hydraulic head has a maximum. That maximum $\ell_T = \ell_{\text{div}} = (\ell_T)_{\text{max}}$ is associated with a maximum sea level $(H_{\text{sea}})_{\text{max}}$. In the flux-control case, their ratio is given analytically and depends only on aquifer parameters, salinity and recharge:

$$(\ell_T)_{\text{max}}/(H_{\text{sea}})_{\text{max}} = [\sin^2\varphi + r/K\delta(1 + \delta)]^{-1/2}. \tag{3}$$

In the head-control case, corresponding $(\ell_T)_{\text{max}}$ and $(H_{\text{sea}})_{\text{max}}$ values are instead determined numerically and depend also on the chosen control-section conditions (since ℓ_{div} depends on those conditions; see SM 1, equation S16 available at stacks.iop.org/ERL/8/014001/mmedia): (a) from the function $\ell_T(H_{\text{sea}})$ for fixed $\phi(\ell_{\text{control}})$ and (b) from the function $\ell_T(\phi_{\text{control}})$ for fixed H_{sea} . An important question regarding these limit values $(\ell_T)_{\text{max}}$ and $(H_{\text{sea}})_{\text{max}}$, addressed further in the results discussion below, is then if, how and under what aquifer conditions those different sea-level rise scenarios approach this H_{sea} -threshold.

Specifically, scenario A1FI of the IPCC (Bates et al 2008) estimates the most severe sea-level rise over the next 100 yr (relative to 1980–99 and excluding future rapid changes in ice flow) at $\Delta H_{\text{sea}} = 0.59$ m. A more recent AMAP (2011) report, however, projects that the sea level may rise by as much as $\Delta H_{\text{sea}} = 1.6$ m in the same 100-yr perspective (sea-level rise projections until 2100 range from 0.9 to 1.6 m, taking into account substantial Arctic ice melting). Our simulations investigate main sea-intrusion implications of both of these sea scenarios. Results are then calculated for variations about a base case configuration for flux-control conditions with $q_0 = -0.4$ m²/day and for head-control conditions with

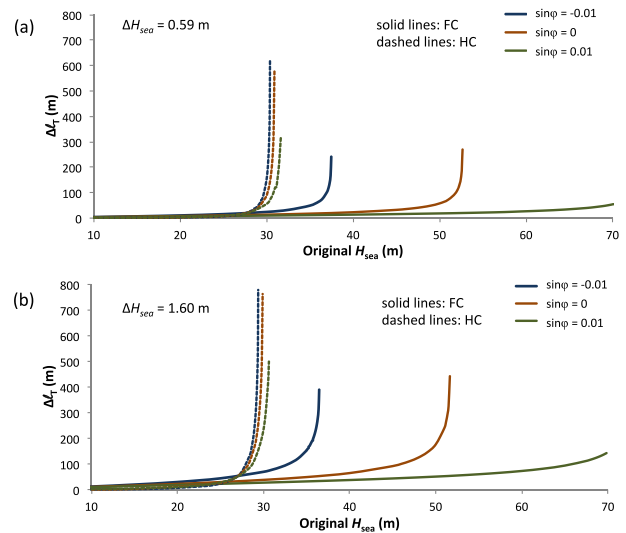


Figure 1. Effect of aquifer slope and sea-level rise on the change of interface toe position $\Delta\ell_T$ as function of original sea level above the aquifer base at the coastline H_{sea} . Results are shown for different aquifer slopes $\sin\varphi$ (-0.01 , 0 , $+0.01$), boundary conditions (flux control, FC, and head control, HC) and sea-level rise (a) $\Delta H_{\text{sea}} = 0.59$ m and (b) $\Delta H_{\text{sea}} = 1.60$ m.

$\phi(\ell_{\text{control}} = 2000 \text{ m}) = 32 \text{ m}$. These control quantities were adopted as *equivalent*, in the sense that they both give $\ell_T \approx 260$ m for the base case, with parameters: bed slope $\sin\varphi = 0.01$, normalized density difference $\delta = (\rho_s - \rho_f)/\rho_f = 0.025$, hydraulic conductivity $K = 10$ m/day and aquifer depth at the coastline $H_{\text{sea}} = 30$ m; the recharge rate was $r = 80$ mm yr⁻¹ in all cases. In all calculations the coastline position remained unchanged, idealizing the coast as vertical; this approximation has also been used in previous seawater intrusion solutions and their applications (e.g., Werner and Simmons (2009)) and does not influence the *trends* of the flow quantities relevant to this study.

3. Results

Figures 1–5 illustrate a sample of the simulation results; tables 1–5 in SM 2 (available at stacks.iop.org/ERL/8/014001/mmedia) provide a more complete summary of parameters and results. In the following we abbreviate flux and head control by FC and HC, respectively. Figure 1 shows the change of the interface toe position ($\Delta\ell_T$) as function of the original coastline depth (H_{sea} , measured from sea level to aquifer base) for different scenarios of sea-level rise (ΔH_{sea}) and aquifer slopes; see SM 2, tables A1a, b (available at stacks.iop.org/ERL/8/014001/mmedia) for the set of parameters and results. Generally, aquifer vulnerability to sea intrusion after sea-level rise (ΔH_{sea}) is greater for deeper aquifers, i.e., greater depth H_{sea} moves the interface toe increasingly inland (greater $\Delta\ell_T$). Full seawater intrusion is imminent, as discussed above, at the sea-level limit $H_{\text{sea}} = (H_{\text{sea}})_{\text{max}}$, for which the resulting toe position after the sea-level rise becomes $\ell_T = (\ell_T)_{\text{max}}$. The illustrated result curves in figure 1 terminate at those maximum toe positions,

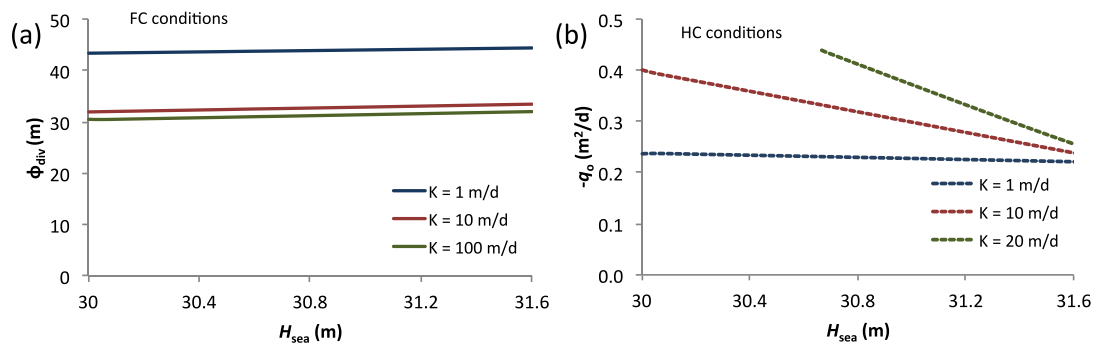


Figure 2. Groundwater hydraulics as functions of sea level $H_{sea} = 30 \text{ m} + \Delta H_{sea}$ after rise ΔH_{sea} . Results are shown for different hydraulic conductivity, K , of the coastal aquifer, in terms of: (a) hydraulic head at the groundwater divide, ϕ_{div} , under flux-control (FC) conditions; and (b) outflow of fresh groundwater, $-q_o$, under head-control (HC) conditions.

where the intrusion toe reaches the groundwater divide position ($\ell_T = \ell_{div}$).

Most importantly, the dependence of $\Delta \ell_T$ on original H_{sea} is highly nonlinear for most conditions shown in figure 1; the only exception is for the example of an upward sloping aquifer ($\sin \varphi = 0.01$) in the FC case. This nonlinearity implies that, for any aquifer slope ($\sin \varphi$), a wide range of quite different sea levels (H_{sea}) imply aquifer conditions that are far from full seawater intrusion, but if the sea level H_{sea} exceeds a certain threshold (e.g., H_{sea} greater than ~ 27 m for all HC conditions shown in figure 1), even a sea level slightly above that implies large sensitivity for any sea-level scenario, yielding large intrusion toe change ($\Delta \ell_T$) up to full sea intrusion.

Aquifer slope is then particularly important under FC conditions, for which a rise of sea level also raises the aquifer free surface, which increases aquifer transmissivity (= hydraulic conductivity \times saturated depth, for a homogeneous aquifer), thereby enhancing seawater intrusion. Even small slope differences (e.g., from $\sin \varphi = 0$ to -0.01 or $+0.01$) change then the maximum sea-level limit ($H_{sea})_{max}$ for full seawater intrusion considerably (from 53 m to 38 m, or 72 m respectively). However, independently of aquifer slope, aquifer vulnerability to full sea intrusion is greatest under HC conditions, for which a sea-level rise also reduces the groundwater outflow to the sea by shifting the groundwater divide towards the coastline (see further SM 2, table A1a, b available at stacks.iop.org/ERL/8/014001/mmedia).

Figure 2 shows the effect of sea-level rise (ΔH_{sea}) on the hydraulic head at the groundwater divide (ϕ_{div} for the FC case) and the groundwater outflow to the sea ($-q_o$ for the HC case) for different aquifer hydraulic conductivity (K); see further parameters and results in SM 2, tables A2a, b (available at stacks.iop.org/ERL/8/014001/mmedia). In the FC case (figure 2(a)), ϕ_{div} is expectedly lower for higher K , as less head differential is needed to ensure the fixed outflow to the sea $-q_o$, and increases linearly with increasing sea-level rise ΔH_{sea} (yielding different sea levels H_{sea} after the rise) in order to sustain the fixed outflow to the sea. Under HC conditions (figure 2(b)), the outflow to the sea ($-q_o = r\ell_{div}$) varies, decreasing linearly with increasing sea level (H_{sea}) over the investigated range, as the groundwater divide location

(ℓ_{div}) moves seawards to maintain the given inland boundary condition $\phi(\ell_{control})$. The fresh groundwater outflow to the sea ($-q_o$) is expectedly higher for higher hydraulic conductivity K , but the levels converge as the groundwater divide moves seawards and the toe approaches the divide with increasing sea level (H_{sea}). In the case of $K = 100 \text{ m d}^{-1}$, which is illustrated for FC conditions in figure 2(a), the same HC condition as for the lower- K cases gives $\ell_{div} > \ell_{control}$ for $H_{sea} < 31.53$ m, i.e., the divide lies outside the solution domain, so its value cannot be known and $-q_o$ cannot be calculated; the same limitation applies also for the illustrated case of $K = 20 \text{ m d}^{-1}$ if $H_{sea} < 30.7$ m.

Figure 3 shows relative sea intrusion, in terms of the ratio between the intrusion toe and groundwater divide positions (ℓ_T/ℓ_{div}) for the FC case, and of the ratio between the intrusion toe and the inland boundary positions ($\ell_T/\ell_{control}$) for the HC case, as function of resulting sea level (H_{sea}) after rise (ΔH_{sea}) for different hydraulic conductivity (K) in the coastal aquifer; see SM 2, tables A3a, b (available at stacks.iop.org/ERL/8/014001/mmedia) for the set of parameters and results. In the FC case, the relative sea intrusion (ℓ_T/ℓ_{div}) is relatively insensitive to sea-level rise (ΔH_{sea}); Chang et al (2011) confirm this finding for a horizontal aquifer. In contrast, in the HC case, the relative sea intrusion ($\ell_T/\ell_{control}$) increases highly nonlinearly with sea-level rise (ΔH_{sea}) for relatively high aquifer conductivity ($K \geq 10 \text{ m d}^{-1}$) and original sea level (H_{sea} of 50 m, figure 3(b)). This nonlinearity implies that an aquifer may remain far from complete sea intrusion for substantial sea-level rise (ΔH_{sea}), but if the resulting sea level (H_{sea}) approaches a threshold (e.g., resulting H_{sea} of ~ 51 m, or $\Delta H_{sea} \approx 1$ m, for $K = 10 \text{ m d}^{-1}$ in figure 3(b)), even a slight further increase in resulting H_{sea} may lead to complete seawater intrusion. A curve of $K = 100 \text{ m d}^{-1}$ is absent from figures 3(a) and (b) for HC for the reasons given above for figure 2, and from figure 3(b) for FC, because $\ell_T/\ell_{div} > 1$ always; for $K = 10 \text{ m d}^{-1}$ in figure 3(b) for HC, $\ell_T = (\ell_T)_{max}$ at $H_{sea} = (H_{sea})_{max} \approx 51.26$ m.

Figure 4 shows how the outflow of fresh groundwater ($-q_o$) in the FC case, and the groundwater head at the inland boundary ($\phi_{control}$) in the HC case affect the change in the intrusion toe position ($\Delta \ell_T$) for different

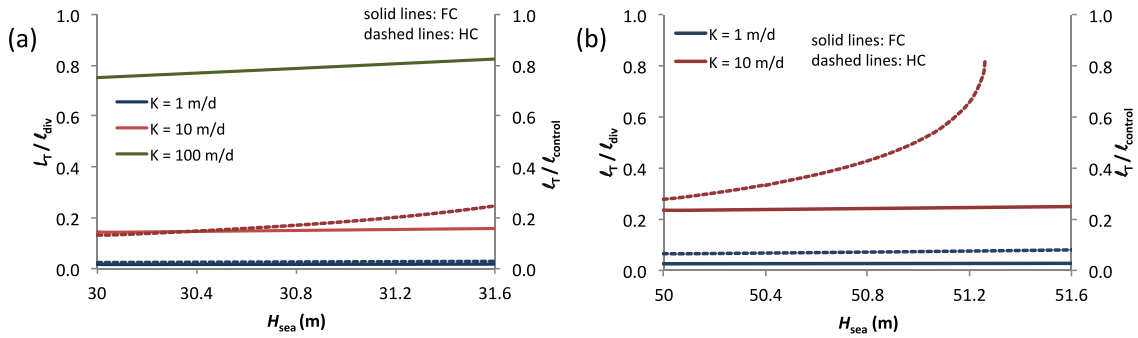


Figure 3. Interface toe position relative to divide position, ℓ_T/ℓ_{div} (left y-axis), in the flux-control (FC) case, and relative to inland boundary, $\ell_T/\ell_{control}$ (right y-axis), in the head-control (HC) case. Results are shown for different K -values, and for different original sea level and sea-level rise ΔH_{sea} : (a) $H_{sea} = 30 \text{ m} + \Delta H_{sea}$ and (b) $H_{sea} = 50 \text{ m} + \Delta H_{sea}$.

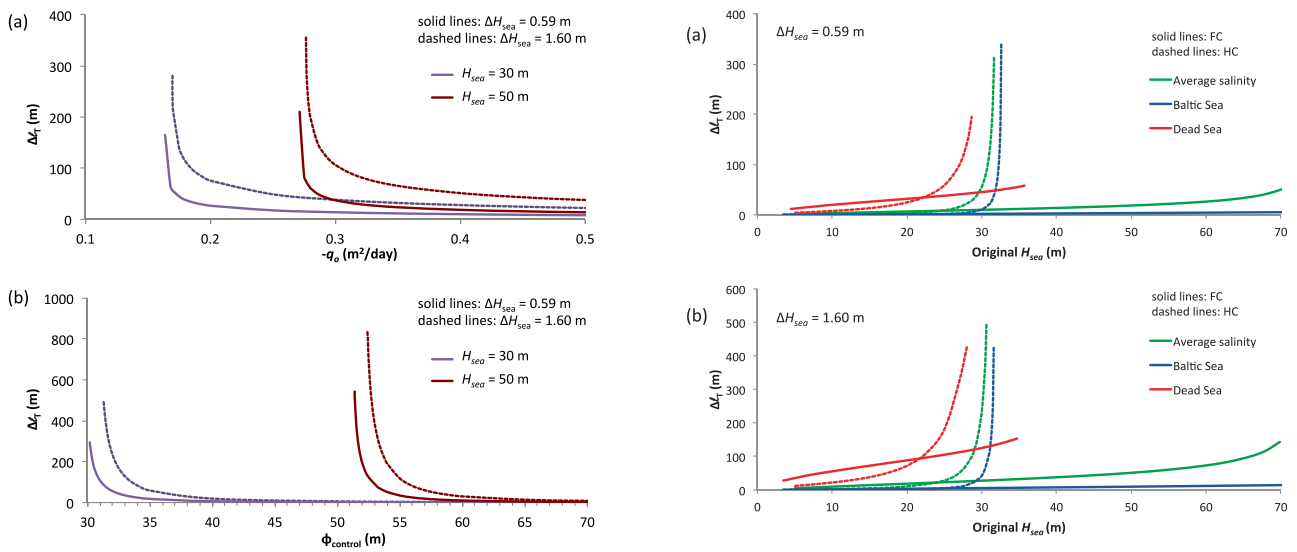


Figure 4. Shift of interface toe, $\Delta \ell_T$, as function of fresh groundwater outflow $-q_o$ (for flux control) and of hydraulic head at the inland boundary $\phi_{control}$ (for head control). Results are shown for different original sea level H_{sea} and sea-level rise ΔH_{sea} .

Figure 5. Shift of interface toe, $\Delta \ell_T$, as function of original sea level H_{sea} for flux-control (FC) and head-control (HC) conditions, and different normalized density difference $\delta = 0.005$ (Baltic Sea), 0.025 (ocean-average salinity and Mediterranean Sea) and 0.187 (Dead Sea) and sea-level rise (a) $\Delta H_{sea} = 0.59 \text{ m}$ and (b) $\Delta H_{sea} = 1.60 \text{ m}$.

scenarios of sea-level rise (ΔH_{sea}) and original sea level (H_{sea}); SM 2, tables A4a, b (available at stacks.iop.org/ERL/8/014001/mmedia) show further parameters and results. The sea-intrusion change ($\Delta \ell_T$) increases nonlinearly with decreasing groundwater outflow ($-q_o$) and inland boundary head ($\phi_{control}$). This nonlinearity is pronounced near tipping points, implying that, if the flow $-q_o$ or the head $\phi_{control}$ is below a certain threshold (e.g., for $\phi_{control}$, of about 35 m and 60 m for original H_{sea} of 30 m and 50 m, respectively, figure 4(b)), even a small decrease in either of them, e.g., by changed groundwater management, can greatly increase the sea-intrusion change ($\Delta \ell_T$), and thereby the aquifer vulnerability to full sea intrusion. Conversely, the sea-intrusion change ($\Delta \ell_T$) can be small even for relative large decrease of groundwater outflow ($-q_o$) or inland boundary head ($\phi_{control}$) if these are maintained above their respective thresholds.

Finally, figure 5 shows how sea-intrusion change ($\Delta \ell_T$) as function of original sea level (H_{sea}) varies with sea salinity, expressed by the normalized density ratios δ ; results are for $\delta = 0.005$ (Baltic Sea), $\delta = 0.025$ (ocean average, also relevant for Mediterranean Sea) and $\delta = 0.187$ (Dead Sea); see SM 2, tables A5a, b (available at stacks.iop.org/ERL/8/014001/mmedia) for complete set of parameters and results. The effect of original sea level (H_{sea}) on sea-intrusion change ($\Delta \ell_T$) after sea-level rise is highly nonlinear for all salinity (δ) values in the HC case, and near-linear in the FC case, for the investigated case of upward sloping aquifer ($\sin \varphi = +0.01$). The nonlinearity in the HC case implies high risk of full seawater intrusion, regardless of sea-level rise ΔH_{sea} and sea salinity, if the original sea level H_{sea} (defined as the aquifer base depth at the coastline below the original sea level) exceeds a threshold value (~ 25 m for all sea conditions in figures 5(a) and (b)).

4. Conclusions

The following major conclusions emerge from this study:

- (1) We have identified high nonlinearity in sea-intrusion responses to sea-level rise, implying important thresholds, or tipping points. If these points are passed, the aquifer responses to sea-level rise shift abruptly from a stable state of mild change responses, to a new stable state of large responses to even small changes that lead rapidly to complete (deep) seawater intrusion. The identified tipping points are of three types:
 - (a) spatial, i.e., a tipping point of aquifer depth (determining the original sea-level depth H_{sea} , figures 1 and 5), determining the particular deeper aquifers or aquifer sections along a coastline with critical risk for full sea intrusion in response to even small sea-level rise;
 - (b) temporal, i.e., a tipping point of critical sea-level change (ΔH_{sea} , figure 3), determining the change magnitude and thereby also the point in time when this change is reached (even though this time cannot be resolved with the present analytical model), beyond which the risk of full sea intrusion in a given aquifer shifts abruptly from low to high;
 - (c) managerial, i.e., a tipping point of critical minimum values of submarine discharge of fresh groundwater or inland groundwater hydraulic head ($-q_0$ or ϕ_{control} , figure 4) that inland water management must maintain in a given aquifer (if needed, through artificial recharge, pumping curtailment, etc) to avoid loss of control and full seawater intrusion in response to even small level rise.
- (2) The existence of high response nonlinearity and associated tipping points depends on aquifer properties (slope, figure 1; hydraulic conductivity, figure 3), and groundwater outflow and hydraulic head conditions ($-q_0$ and ϕ_{control} , figure 4) that may be controlled by inland water management, in combination with sea conditions (sea-level change ΔH_{sea} addressed in all figures, and normalized density ratio δ in figure 5). It is important to recognize the importance of the management-controlled conditions and changes (as did Ferguson and Gleeson (2012) in their recent study of only horizontal aquifer and head-control conditions), as well as of the larger-scale sea conditions and climate-driven changes in view of the present findings of high nonlinearity and tipping points in sea-intrusion responses to these changes.
- (3) Of the control conditions adopted as *equivalent in terms of initial seawater intrusion*, the *flux-control* case is far more resilient to sea intrusion than the *head-control* case, implying that the fresh groundwater outflow must be primarily controlled in order to control sea intrusion, and should therefore be the focus of groundwater management in coastal aquifers.
- (4) The generalized analytical model of interface flow of Koussis et al (2012), which accounts for the aquifer base slope, is useful for parsimonious quantification

and screening of sea-intrusion risks and tipping points under the combination of spatio-temporally variable aquifer, groundwater hydraulics and water management conditions and relatively homogeneous sea conditions prevailing in different aquifer (sections) along extended coastlines.

References

- AMAP 2011 *Snow, Water, Ice and Permafrost in the Arctic (SWIPA): Climate Change and the Cryosphere* (Oslo: Arctic Monitoring and Assessment Programme (AMAP))
- Bates B C, Kundzewicz Z W, Wu S and Palutikof J P (ed) 2008 *Climate change and water Technical Paper of the Intergovernmental Panel for Climate Change* (Geneva: IPCC Secretariat)
- Brown K, Tompkins E L and Adger W N 2002 *Making Waves: Integrating Coastal Conservation and Development* (London: Earthscan)
- Carrera J, Hidalgo J J, Slooten L J and Vázquez-Suñé E 2010 Computational and conceptual issues in the calibration of seawater intrusion models *Hydrogeol. J.* **18** 131–45
- Chang S W, Clement T P, Simpson M J and Lee K 2011 Does sea-level rise have an impact on saltwater intrusion? *Adv. Water Resour.* **34** 1283–91
- Custodio E 1987a Salt-fresh water interrelationship under natural conditions *Groundwater Problems in Coastal Areas* (Paris: UNESCO-IHP)
- Custodio E 1987b Effect of human activities on salt-freshwater relationships in coastal aquifers *Groundwater Problems in Coastal Areas* (Paris: UNESCO-IHP)
- Custodio E and Bruggeman G A 1987 *Groundwater Problems in Coastal Areas: A Contribution to the International Hydrological Programme* (Paris: UNESCO-IHP)
- Destouni G, Shibuo Y and Jarsjö J 2008 Freshwater flows to the sea: spatial variability, statistics and scale dependence along coastlines *Geophys. Res. Lett.* **35** L18401
- Ferguson G and Gleeson T 2012 Vulnerability of coastal aquifers to groundwater use and climate change *Nature Clim. Change* **2** 342–5
- Girinskii N K 1947 Kompleksnyi potentsial potoka presnykh vod so slabo naklonennymi struikami, fil' truyushchevgo v vodopronitsaemoi tolshche morskikh poberezhii *Dokl. Akad. Nauk. SSSR* **58** 559–61
- Jarsjö J and Destouni G 2004 Groundwater discharge into the Aral Sea after 1960 *J. Mar. Syst.* **47** 109–20
- Koussis A D, Mazi K and Destouni G 2012 Analytical single-potential, sharp-interface solutions for regional seawater intrusion in sloping unconfined coastal aquifers, with pumping and recharge *J. Hydrol.* **416/417** 1–11
- Koussis A D et al 2010a Cost-efficient management of coastal aquifers via recharge with treated wastewater and desalination of brackish groundwater: general framework *Hydrol. Sci. J.* **55** 1217–33
- Koussis A D et al 2010b Cost-efficient management of coastal aquifers via recharge with treated wastewater and desalination of brackish groundwater: application to the Akrotiri Basin and Aquifer Cyprus *Hydrol. Sci. J.* **55** 1234–45
- Prieto C and Destouni G 2011 Is submarine groundwater discharge predictable? *Geophys. Res. Lett.* **38** L01402
- Shibuo Y, Jarsjö J and Destouni G 2006 Bathymetry-topography effects on saltwater-fresh groundwater interactions around the shrinking Aral Sea *Water Resour. Res.* **42** W11410
- Strack O D L 1976 A single-potential solution for regional interface problems in coastal aquifers *Water Resour. Res.* **12** 1165–74
- Werner A D and Simmons C T 2009 Impact of sea-level rise on sea water intrusion in coastal aquifers *Ground Water* **47** 197–204